The effects of plasma-processing conditions on the morphology of adherent human blood platelets

R. Murugesan,[1] E. Hanley,[1] R. M. Albrecht,[2] J. A. Oliver,[3] J. A. Heintz,[2] J. L. Lauer,[1] and J. L. Shohet[1,a)]

[1]*Plasma Processing and Technology Laboratory and Department of Electrical and Computer Engineering, University of Wisconsin-Madison, Madison, Wisconsin 53706, USA*
[2]*Department of Animal Sciences, University of Wisconsin-Madison, Madison, Wisconsin 53706, USA*
[3]*Department of Biological Sciences, University of Wisconsin-Milwaukee, Milwaukee, Wisconsin 53206, USA*

(Received 24 December 2007; accepted 19 February 2008; published online 2 May 2008)

Hematocompatibility and nonfouling properties of materials are crucial for the development of small-scale biomedical devices. This study examines the adhesion and morphology of purified human platelets on plasma-polymerized tetraglyme-coated glass substrates. The effect of varying the plasma-processing parameters on platelet responses was determined using scanning electron microscopy. Images of platelets on the coated surfaces show that a significant reduction in platelet adhesion and spreading can be achieved as the processing parameters are varied. © *2008 American Institute of Physics*. [DOI: 10.1063/1.2908200]

I. INTRODUCTION

Biomedical devices that will be in contact with blood require that the blood-contacting surfaces be hematocompatible.[1] Such nonfouling surfaces have been created by the deposition of tetraethylene glycol dimethyl ether $(CH_3O(CH_2CH_2O)_4CH_3)$, i.e., tetraglyme, using radio-frequency (rf) plasma polymerization.[2–4] This results in the formation of a polyethylene-glycol (PEG)-like coating, which resists protein adsorption and cell adhesion.[5] Protein adsorption is usually undesirable because it leads to bacterial adhesion, platelet adhesion, and spreading, as well as thrombus formation.[6–8] It should be noted that PEG is a nontoxic substance, and it is approved by the U.S. Food and Drug Administration for use in biotechnology and consumer applications.

This work investigates the adhesion and morphology of human blood platelets on tetraglyme plasma-polymerized surfaces. The tetraglyme is polymerized on glass substrates in a plasma reactor. We consider the effects of the variation of the plasma-processing parameters on the platelets that adhere to the surfaces. To this end, we have investigated three processing parameters (input power, chamber pressure, and treatment duration) which we have found generate surfaces whose properties differ from each other.

Each surface is exposed to human blood platelets. Following platelet exposure, scanning electron microscope (SEM) images are obtained. The SEM images show the adherent platelets on each surface. The platelets are categorized based on their morphology.[9,10] We measure the percentage of adherent platelets that have morphologies consistent with reduced levels of surface activation. It is hypothesized that surfaces demonstrating low levels of platelet adherence and platelet surface activation will have greater potential for biomedical applications. This work shows that plasma-processing parameters have a significant effect on adhered platelet morphology. Using statistical methods, we have identified which processing parameters are most influential in producing optimized conditions resulting in desirable platelet morphologies.

II. PLASMA POLYMERIZATION REACTOR

The plasma-polymerization reactor used in this work is shown in Fig. 1. A glass chamber (length of 45 cm and internal diameter of 12 cm) is wrapped externally with two grounded electrode straps. A powered electrode is placed between the grounded electrodes. The chamber is closed on both ends by metal flanges, which are also grounded. The electrodes are coupled to a 13.56 MHz rf source with a matching network. A mass-flow controller regulates the flow of the argon carrier gas and tetraglyme vapor into the chamber. A throttle valve is placed at the output of the processing chamber in order to vary the fraction of tetraglyme and the pressure in the chamber. Argon can flow either directly into the chamber through the main feed line or through the flask containing the vaporized liquid tetraglyme and then into the chamber via the main feed line. At room temperature, tetraglyme is a liquid. As a result, the tetraglyme was vaporized by placing the flask in a heating mantle. To prevent the tet-

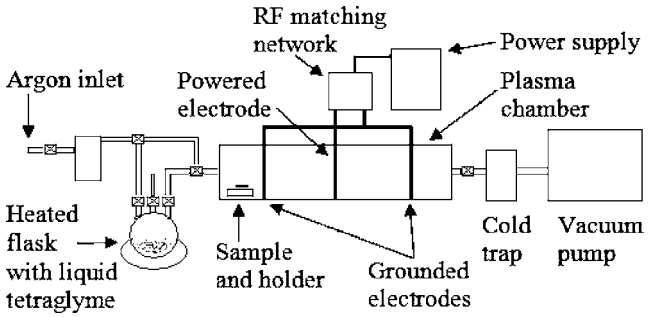

FIG. 1. Plasma polymerization reactor.

a)Author to whom correspondence should be addressed. Electronic mail: shohet@engr.wisc.edu.

raglyme from condensing on the feed line, it was heated to 125 °C. A liquid-nitrogen cold trap is placed between the chamber output and the vacuum pump.

III. PLASMA TREATMENT

Before plasma polymerization, the flask, containing 10 ml of liquid tetraglyme, was degassed four times using liquid nitrogen. After a substrate was mounted in the chamber, it was evacuated and the flask and feed line were heated. The chamber was then purged with argon gas for 5 min at a pressure of 200 mTorr without producing plasma. The reactor was then discharged cleaned by generating an argon plasma for 5 min at an incident power of 800 W at the same pressure.

After the completion of discharge cleaning, the tetraglyme was vaporized by heating it to 110 °C. The valve connecting the flask to the chamber was opened, and the argon carrier gas was fed into the flask. The steady-state chamber pressure was varied between 50 and 200 mTorr by adjusting either the mass-flow controller voltage (to change the flow of argon and tetraglyme into the chamber) or by adjusting the throttle valve (to change the flow rate of argon and tetraglyme monomer leaving the chamber).

Once the desired steady-state pressure inside the chamber was reached, the rf power supply was turned on and slowly increased to a given incident power to create the tetraglyme/argon plasma. The samples were exposed to the plasma for times between 20 and 40 min. After the plasma-polymerization procedure was completed, the rf power was slowly decreased to zero and the valve connecting the flask to the chamber was closed. The vacuum pump was turned off and the chamber was slowly vented to atmospheric pressure. The plasma-polymerized samples were then removed from the chamber and soaked in liquid methanol overnight. This step ensured that any plasma-polymerized tetraglyme fragments that were not bonded to the surface were removed. After each processing operation, the chamber was cleaned with methanol to remove as much tetraglyme as possible that was deposited onto the chamber walls before subsequent samples were plasma polymerized.

IV. PLATELET PREPARATION AND SURFACE EXPOSURE

Purified platelets were prepared from normal human blood.[11] Blood was collected from healthy donors with no recent history of aspirin use. The blood was anticoagulated with the addition of 0.5 ml of a 3.2% buffered citrate solution to 9.5 ml of whole blood. The blood was centrifuged for 15 min at an acceleration of 110 g. The platelet-rich plasma was then run through a gel filtration column composed of Sepharose CL-2B beads in Hepes Tyrode's buffer. 1 ml volumes of the platelet-rich fraction were collected from the column. After the gel filtration process, the calcium concentration was brought up to 3 mM to provide sufficient calcium for normal platelet activity. Platelet concentrations were adjusted to 192 000 platelets/μl.

The plasma-treated glass substrates were placed in a 9 cm diameter polystyrene Petri dish. One droplet of the platelet solution was placed on the surface of each substrate with a pipette. The surfaces were allowed to remain at 100% relative humidity in a static state for 20 min at room temperature (25 °C). The platelet solution was then withdrawn from each substrate surface with the pipette, and the sample was immediately dipped in a beaker containing warm (37 °C) phosphate buffered solution (PBS). Following the buffer wash, the samples were fixed by placing them overnight in another Petri dish containing a mixture of 1.25% glutaraldehyde and 1% w-v tannic acid in a 0.1 mol phosphate buffer.

The samples were then individually dipped in a beaker containing fresh PBS and transferred to another Petri dish. They were then dehydrated via an ethanol series with 5 min exchanges in 10 ml ethanol concentrations of 30%, 50%, 70%, 80%, 90%, 95%, and 100% ethanol. The final concentration was 100% ethanol by volume.

Following dehydration, the samples were dried with the critical-point procedure with molecular-sieve-dried 100% ethanol as the intermediate fluid and liquid carbon dioxide as the transitional fluid (Tousimis Samdri 780). The dried samples were sputter coated with an approximately 10 nm thick conductive coating of 60:40 gold-palladium alloy (SeeVac Auto Conductavac IV). The sputtering process utilised an argon gas dc discharge with a current of 30 mA, a pressure of 120 mTorr, and a sputtering duration of 3 min.

The surfaces were examined with an SEM (Hitachi S-570). At an accelerating voltage of 10 kV, images were obtained at different magnifications in the central region of each sample's surface.

V. RESULTS AND DISCUSSION

A. Platelet morphology

Prior to activation, the human blood platelet is discoid in shape. Upon activation, it exhibits a progression of morphologies from discoid to spherical to dendritic to fully spread forms.[12,13] These morphologies are summarized in Table I (Refs. 14–16) with their corresponding SEM images shown in Fig. 2. Figure 2(a) shows the unactivated discoid phase, which progresses to the fully spread stage shown in Fig. 2(e). Figure 2(f) shows the morphology of a nonviable platelet that does not follow the normal progression if the surface is toxic to platelets. Figure 2(g) shows a platelet that has died after reaching the fully spread stage.

It is known that the state of activation of adherent platelets on a polymer surface is a factor that is related to the hematocompatibility of the surface.[17] Since platelet activation can ultimately result in thrombus formation on blood-contacting surfaces and the associated restriction of blood flow,[18] ideally it should not occur on the surfaces of biomaterials. Therefore, surfaces on which there is minimal or no platelet adhesion are desirable. However, it is extremely difficult to eliminate all platelet adhesion. Thus, on surfaces where platelet adhesion does occur, those that possess the highest fraction of unactivated or minimally activated platelets, i.e., discoid/spherical platelets, can be considered more suitable for biological applications.

TABLE I. Morphology of adherent platelets.

Discoid/spherical	The platelet is not activated or is in the very early stages of activation and has not started spreading. This morphology is similar to the platelet's *in vivo* state.
Dendritic	One or more pseudopodia are present, and no flattening is evident.
Spreading dendritic	One or more pseudopodia are flattened, and the hyaloplasm has not spread between the pseudopodia.
Spreading	The hyaloplasm has partially spread.
Fully spread	The hyaloplasm has extensively spread, and there are no distinct pseudopodia.
Dendritic nonviable	The nonviable platelet is arrested in the dendritic phase; the platelet extends a few long, thin pseudopodia and then contracts to leave a swollen, rounded body.
Spreading nonviable	The platelet initially spreads normally but eventually swells and contains randomly moving intracellular components.

The variation in the numbers of platelets adhering to the surface may be very high.[19] In any case, the morphological fraction of platelets in each of the seven states listed in Table I can be used as a significant measure of the degree of hematocompatibility or likelihood of leading to thrombus formation. Accordingly, the platelets observed on the obtained SEM images were classified into each of the seven morphological states described in Table I.

B. Design matrix

To elucidate the effects of the plasma-processing parameters on platelet morphology, a two-level three-factor factorial experimental design was performed. As mentioned earlier, the three factors are the following plasma-processing parameters: incident power, chamber pressure, and treatment duration. These factors where chosen because they can be easily controlled and resulted in measurable differences in platelet-adhesion properties.

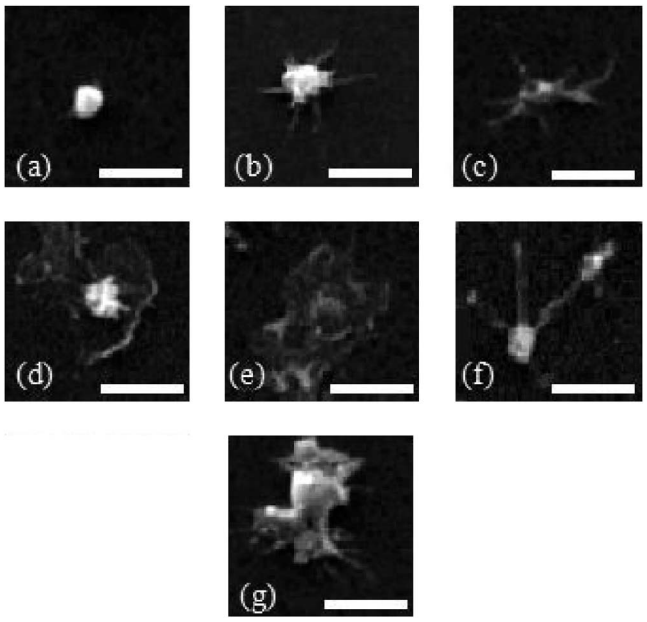

FIG. 2. Types of platelet morphology on surfaces: (a) discoid, (b) dendritic, (c) dendritic spreading, (d) spreading, (e) fully spread, (f) dendritic nonviable, and (g) spreading nonviable. The bar represents 10 μm.

Samples 1–16 are plasma-polymerized surfaces on glass substrates. Samples 17 and 18 are untreated glass substrates used as a control, while samples 19 and 20 are silicon-dioxide surfaces also used as a control. Two surfaces (replicates) were produced for each processing condition as shown in Table II, the matrix for the experimental design. The first column in Table II identifies the condition number which is used for identification purposes in the analysis. Columns 3–5 show the design matrix of processing conditions.

C. Analysis of SEM images

The morphology of the platelets seen on the SEM images obtained at 1000× magnification was analyzed by manually classifying each platelet seen on the images into one of the seven morphological categories described in Table

TABLE II. Design matrix and the results of the morphological analysis.

Condition number	Sample number	Incident power (W)	Chamber pressure (mTorr)	Treatment duration (min)	Adherent discoid/spherical platelets averaged over both replicates (%)	Standard deviation of the replicates (%)
1	1, 2	200	50	20	21	±6
2	3, 4	200	50	40	72	±6
3	5, 6	200	100	20	4	±1
4	7, 8	200	100	40	4	±1
5	9, 10	800	50	20	14	±6
6	11, 12	800	50	40	11	±3
7	13, 14	800	100	20	14	±3
8	15, 16	800	100	40	1	±1
9	17, 18	Glass control surfaces			3	±2
10	19, 20	Silicon dioxide control surfaces			0	±0

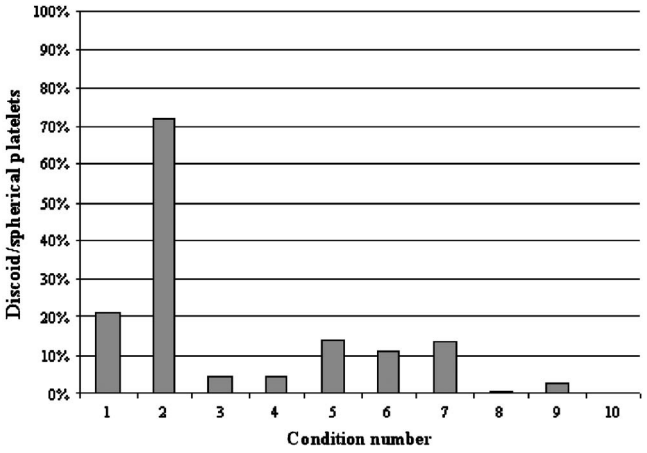

FIG. 3. Percentage of platelets with discoid/spherical morphology vs condition number.

I. The total number of platelets on each image was obtained by adding the number of platelets in each of the individual categories.

Since as described in the previous section, discoid/spherical platelets represent the least-destructive morphology for biological applications, the percentage of discoid/spherical platelets on every image was calculated as a function of the total number of platelets and averaged over both replicates for each treatment condition; the results are shown in the sixth column of Table II. The standard deviation of these data is shown in the last column.

Figure 3 shows the percentage of adherent discoid/spherical platelets (averaged over both replicates) for each processing condition shown in Table II. Condition 2 shows a remarkable improvement. This improvement can be qualitatively understood by comparing Figs. 4(a) and Fig. 4(b). Figure 4(a) shows a 1000× SEM image of a control surface, and Fig. 4(b) shows a 1000× SEM image of a surface treated under condition 2. In Fig. 4(a), most of the adherent platelets are in advanced stages of activation, and the percentage of discoid/spherical platelets is relatively low. In contrast, most of the adherent platelets in Fig. 4(b) have a discoid/spherical morphology. Figure 4(c) shows a higher magnification SEM image of the surface shown in Fig. 4(b). In this figure, a platelet in the "spreading" stage is at the center, and to its left is a discoid/spherical platelet.

D. Statistical analysis

In order to determine the relative effect of each plasma-processing parameter on the percentage of discoid/spherical platelets, a statistical analysis[20] was completed by comparing the percentage of discoid/spherical platelets on each sample. The analysis produced two types of results as shown in Table III. These are (1) the main or interactive effects and (2) the percent contribution of a given factor or combination of factors to the results.

The effect of each variable or variables is expressed as a percentage in Table III. For example, if the exposure duration to the plasma is increased, Table III states that there is an 8% increase in the percentage of discoid/spherical platelets observed, whereas if the pressure is increased, there is a 24% decrease in the percentage of discoid/spherical platelets observed. The 95% confidence interval of the effects was determined to be +15%.

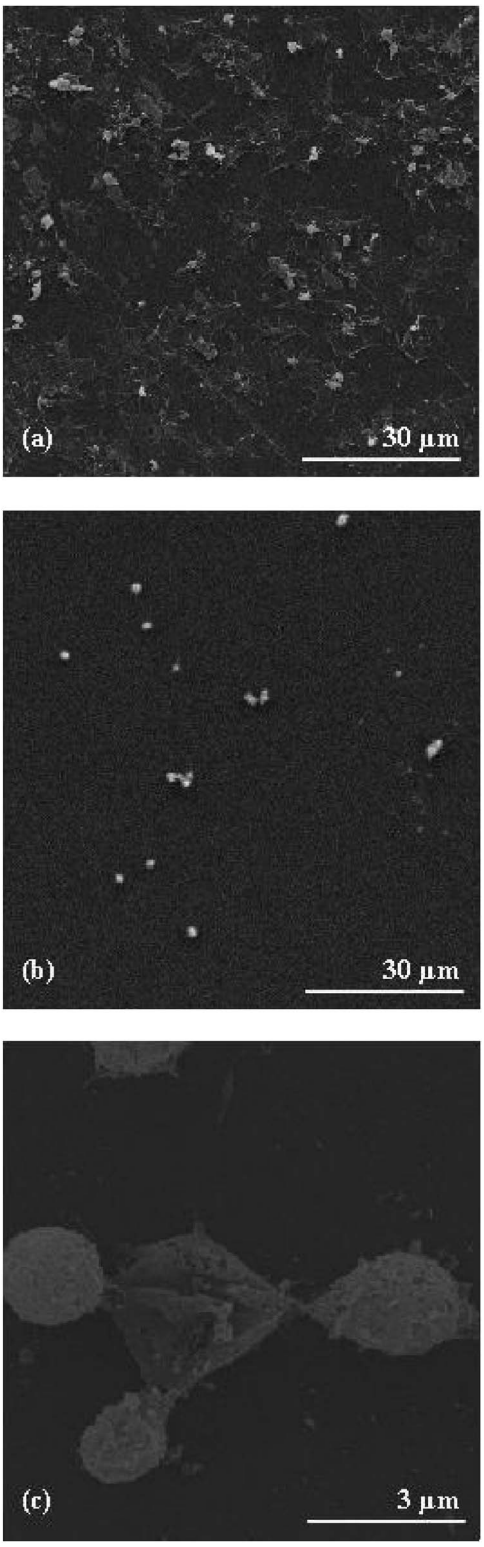

FIG. 4. SEM images of (a) a control silicon dioxide surface (sample 19), obtained at 1000× magnification, (b) a surface processed under condition 2 (sample 3), obtained at 1000× magnification, and (c) a surface processed under condition 2 (sample 4), obtained at 1000× magnification.

The right-hand column in Table III lists the percent contribution of each factor (or combination of factors) to the percentage of discoid/spherical platelets. Ideally, the sum of

TABLE III. Statistical analysis of the three plasma-processing parameters.

Factor(s)	Effect (%)	Contribution (%)
Duration	8	4
Pressure	−24	39
Power	−16	16
Duration and pressure	−15	14
Duration and power	−17	17
Pressure and power	19	24
Duration, power and pressure	9	6

each of the percentages in the contribution column should add up to 100%. However, because of statistical uncertainties, the error margin in the percentages for the contributions was +22%, resulting in a sum greater than 100%.

VI. CONCLUSIONS

In summary, we have shown that the morphology of platelets adhering to plasma-treated surfaces is strongly dependent on the plasma-processing conditions. From Table III, the most significant factors affecting the fraction of discoid/spherical morphology and whose effects and contributions are greater than the error ranges are the pressure and pressure and power factors. Furthermore, it was found that the percentage of adherent discoid/spherical platelets, which are the most desirable from the point of view of the hematocompatibility of the surface, can be varied from 1% to 72%. However, because such a wide range of results that can be obtained, it is critical that processing conditions be optimized for successful synthesis of an effective biomaterial.

[1]Q. J. Lai, S. L. Cooper, and R. M. Albrecht, "Thrombus formation on artificial surfaces: Correlative Microscopy," Proceedings of the 12th International Congress for Electron Microscopy, Seattle, WA, 1990, Vol. 3, p. 840.
[2]G. P. Lopez, B. D. Ratner, C. D. Tidwell, C. L. Haycox, R. J. Rapoza, and T. A. Horbett, J. Biomed. Mater. Res. **26**, 415 (1992).
[3]M. Shen, L. Martinson, M. S. Wagner, D. G. Castner, B. D. Ratner, and T. A. Horbett, J. Biomater. Sci., Polym. Ed. **13**, 367 (2002).
[4]M. Shen, M. S. Wagner, D. G. Castner, B. D. Ratner, and T. A. Horbett, Langmuir **19**, 1692 (2003).
[5]M. Zhang, T. Desai, and M. Ferrari, Biomaterials **19**, 953 (1998).
[6]H. Elwing, Biomaterials **19**, 397 (1998).
[7]D. Kiaei, A. S. Hoffman, and T. A. Horbett, in *Proteins at Interface II*, edited by J. L. Brash and T. A. Horbett (American Chemical Society, Washington, DC, 1995), pp. 450–462.
[8]J. M. Anderson, T. L. Bonfield, and N. P. Zaits, Int. J. Artif. Organs **13**, 375 (1990).
[9]S. L. Goodman, K. S. Tweden, and R. M. Albrecht, Cells Mater. **5**, 15 (1995).
[10]S. L. Goodman, K. S. Tweden, and R. M. Albrecht, J. Biomed. Mater. Res. **32**, 249 (1998).
[11]J. A. Oliver, D. M. Monroe, F. C. Church, H. R. Roberts, and M. Hoffman, Blood **100**, 539 (2002).
[12]R. D. Allen, L. R. Zacharski, S. T. Widirstky, R. Rosenstein, L. M. Zaitlin, and D. R. Burgess, J. Cell Biol. **83**, 126 (1979).
[13]S. L. Goodman, T. G. Grasel, S. L. Cooper, and R. M. Albrecht, J. Biomed. Mater. Res. **23**, 105 (1989).
[14]M. I. Barnhardt, R. T. Walsh, and J. A. Robinson, Ann. N.Y. Acad. Sci. **201**, 360 (1972).
[15]S. L. Goodman, M. D. Lelah, L. K. Lambrecht, S. L. Cooper, and R. M. Albrecht, Scan Electron Microsc. **1**, 279 (1984).
[16]L. M. Waples, O. E. Olorundare, S. L. Goodman, Q. J. Lai, and R. M. Albrecht, J. Biomed. Mater. Res. **32**, 65 (1998).
[17]J. I. Sheppard, W. G. McClung, and I. A. Feuerstein, J. Biomed. Mater. Res. **28**, 1175 (1994).
[18]R. K. Andrews, J. A. López, and M. C. Berndt, Int. J. Biochem. Cell Biol. **29**, 91 (1997).
[19]J. H. Lee, B. J. Jeong, and H. B. Lee, J. Biomed. Mater. Res. **34**, 105 (1998).
[20]D. C. Montgomery, *Design and Analysis of Experiments*, 6th ed. (Wiley, New York, 2005).